PCCP

On the HCl and DCl complexes of methylenecyclopropane in liquid argon†

Roman Szostak,‡ Wouter A. Herrebout and Benjamin J. van der Veken*

Department of Chemistry, Universitair Centrum Antwerpen, Groenenborgerlaan 171, B-2020 Antwerpen, Belgium

Received 21st June 2000, Accepted 18th July 2000
Published on the Web 16th August 2000

The formation of weak molecular complexes between methylenecyclopropane (MeCP) and HCl or DCl dissolved in liquid argon and liquid nitrogen has been investigated using infrared spectroscopy. Evidence was found for the formation of a 1 : 1 complex in which the HCl molecule binds to the C=C double bond. Weaker bands due to the two different 1 : 2 complexes derived from the 1 : 1 complex were observed. From spectra recorded at different temperatures between 90 and 130 K, the complexation enthalpy for the 1 : 1 complex formed was determined to be $-9.9(3)$ kJ mol^{-1}, while the corresponding value for the most stable 1 : 2 complex, MeCP · HCl · HCl, was determined to be $-14.6(4)$ kJ mol^{-1}. Structural and spectral information for the 1 : 1 and the 1 : 2 complexes was obtained from DFT calculations at the B3LYP/6-311++G(d,p) level. Using free energy perturbation Monte Carlo simulations to calculate the solvent influences, and statistical thermodynamics to account for zero-point vibrational and thermal contributions, the complexation energies for the 1 : 1 complex and the 1 : 2 complex were estimated from the experimental complexation enthalpies to be $-16.9(12)$ and $-28.7(14)$ kJ mol^{-1}. These numbers are compared with single-point energies calculated at the MP2/aug-cc-PVTZ level.

Introduction

The complexes between hydrogen halides and π- or pseudo-π bonds are of interest both as model systems for weakly interacting species and as precursors for the reaction between the two molecules, which is believed to be initiated by the activation of the base molecule by its acid counterpart in the complex. The simplest complex of hydrogen chloride with a π-bond system, *i.e.* with ethene, has been intensively studied by a variety of methods, including matrix-isolation IR spectroscopy,[1,2] FT-microwave spectroscopy[3,4] and cryospectroscopy.[5,6] The stability of the 1 : 1 bonded complex in liquid argon (LAr), expressed as a complexation enthalpy ΔH°, was determined to be $-8.7(3)$ kJ mol^{-1}.[6]

The C–C bonds in cyclopropane are highly strained, and therefore, are regarded as pseudo-π bonds. Its complex with HCl has also been described.[7,8] Intuition might suggest that the electron donor characteristics of a pseudo-π bond are weaker than that of a π bond itself, from which would be anticipated that the cyclopropane complex is significantly weaker than the ethene complex. However, the complexation enthalpy in LAr of the former has recently been determined to be $-7.0(4)$ kJ mol^{-1},[9] which is remarkably close to the value for $C_2H_4 \cdot HCl$.

In MeCP, both types of electron donors are present, and the above complexation enthalpies suggest that this compound could exhibit an interesting complexation pattern with both types of complexes being formed simultaneously. In the experimental studies reported so far, including matrix isolation spectra[10] and jet expansion microwave spectra,[11–13] however, only the complex with the π bond has been identified. These studies have investigated the complexes in solid matrices and in molecular beams, *i.e.* under non-equilibrium conditions, and it cannot be excluded that in these experiments kinetic factors determine which type of complex prevails. Therefore, it was judged of interest to study the complexes between MeCP and HCl under equilibrium conditions. In view of the weakness of the complexes, they must be studied at low temperatures. The approach followed here is the IR study of mixtures of the monomers dissolved in LAr and liquid nitrogen, as these solvents create a weakly-interacting cryogenic environment, ideally suited for IR investigation, in which the formation of weak complexes is easily detected.[14,15]

At the outset it may be remarked that, in terms of nucleophilicities of the donor sites, MeCP is not simply the sum of ethene and cyclopropane, as in MeCP the properties of each type of donor undoubtedly are influenced by the vicinity of the other type. Insight into this was gained through *ab initio* calculations of all conceivable complexes. In the following paragraphs we will first discuss the results of these calculations. Subsequently, the IR spectra will be used to determine the number of observed complexes, their stoichiometry, their geometry and stability. It will be shown that in the cryosolutions also, a single type of 1 : 1 complex is being formed, in which the HCl molecule binds to the C=C double bond. In addition, evidence for the formation of two different 1 : 2 complexes will be reported.

Experimental

The sample of MeCP was purchased from Fluka (FLUKA 66765, stated purity >99%) and was purified immediately prior to use by low-temperature, low-pressure fractionation. HCl and DCl were synthesized in small amounts by hydrolyzing PCl_3 with H_2O and D_2O, respectively, and were purified by pumping the reaction mixtures through a 180 K slush, followed by low-temperature, low-pressure fractionation. The

† Electronic Supplementary Information available. See http://www.rsc.org/suppdata/cp/b0/b004965o/

‡ Present address: Department of Chemistry, University of Wrocław, F. Joliot-Curie 14, 50-383 Wrocław, Poland.

solvent gases argon and nitrogen were obtained from l'Air Liquide and had stated purities of 99.9999%.

All spectra were recorded using a Bruker IFS 113v or a Bruker 66v Fourier Transform spectrometer. For the mid-IR (4000–400 cm^{-1}) spectra, a Globar source was used in combination with a Ge/KBr beamsplitter and a liquid nitrogen cooled broadband MCT detector. For the far-IR spectra (300–10 cm^{-1}) several Mylar beamsplitters were used in combination with a liquid helium cooled silicon bolometer. The interferograms were averaged over 200 scans, Happ–Genzel apodized and Fourier transformed using a zero filling factor of 4, to yield spectra at a resolution of 0.5 cm^{-1}.

The experimental setup consists of a pressure manifold needed for filling and evacuating the cell and for monitoring the amount of gas used in a particular experiment, and the actual cell. The cell has an optical path length of 7 cm and is equipped with slightly wedged Si windows that are held in high-pressure window holders.[16] The cell can withstand an internal pressure of at least 150 bar at 77 K without leaking. To be able to distinguish the spectra of dissolved and undissolved species, for MeCP a solid state spectrum was obtained by condensing a small amount of the compound onto a CsI window, cooled to 10 K using a Leybold Heraeus ROK 10-300 cooling system, followed by annealing until no further changes were observed in the IR spectrum.

Computational details

The density functional theory (DFT) calculations were performed using GAUSSIAN 98.[17] For all calculations, Becke's three-parameter exchange functional[18] was used in combination with the LYP correlation functional,[19] while the 6-311++G(d,p) basis set was used throughout as a compromise between accuracy and applicability to larger systems. To reduce the errors arising from the numerical integration, for all calculations the *finegrid* option, corresponding to roughly 7000 grid points per atom was used.

The complexation energies were calculated by subtracting the energies of the monomers from those of the complexes, and these energies were corrected for basis set superposition error (BSSE) using the counterpoise method of Boys and Bernardi.[20] For all equilibrium geometries, vibrational frequencies and IR intensities were calculated using standard harmonic force fields.

Results

A. *Ab initio* calculations

Because of its structure, MeCP is expected to show three possible interaction sites, of different nucleophilicity: Lewis acids can interact with MeCP through the exocyclic π-bond, and with the 1–2 and 2–3 cyclopropyl bonds. Calculations based on the Buckingham–Fowler model,[21–23] however, predict that for MeCP · HCl and MeCP · HF only two different stable complexes occur, a more stable isomer in which the HX molecule is bonded to the π bond, and a less stable one with the hydrogen halide bonded to the 2–3 cyclopropyl bond. For none of the complex species studied experimentally, has theoretical data based on *ab initio* molecular orbital calculations been reported. Therefore, to gain insight into the structures and stabilities of the different 1 : 1 and 1 : 2 complexes between MeCP and HCl, geometry optimizations were carried out starting from different relative positions of the molecules involved. The resulting equilibrium geometries for the 1 : 1 complex are shown in Fig. 1. The complexation energies ΔE, the corresponding values for the BSSEs, E_{BSSE}, and the BSSE corrected complexation energies ΔE_{corr} are collected in Table 1. The structural parameters can be evaluated from the equilibrium cartesian coordinates that are listed in Table S1† of the supplementary material. Because of the large number of internal coordinates involved no detailed description of the calculated equilibrium geometries will be reported.

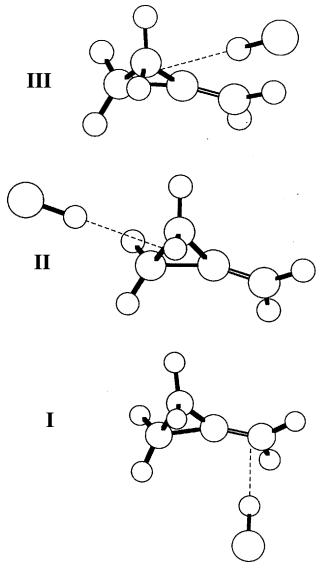

Fig. 1 B3LYP/6-311++G(d,p) equilibrium geometries for the different 1 : 1 complexes formed between MeCP and HCl.

In the 1 : 1 complexes **I**–**III** the interaction occurs through each of the three sites on MeCP. In the π complex **I** the HCl is interacting with the C=C double bond, and is situated in a plane perpendicular to the heavy atom plane of MeCP. In the γ complexes **II** and **III** the HCl interacts with C–C bonds of the ring, and for each of these the HCl molecule is situated in the heavy atom plane of MeCP, in agreement with experiment.[11] Inspection of the complexation energies listed in Table 1 shows that the π complex **I** is the global minimum, while the complexes **II** and **III**, involving the 2–3 and 1–2 bond in the ring, respectively, are at increasingly higher energy.

In Table 1 the complexation energies for the ethene complex, $C_2H_4 \cdot HCl$, and the cyclopropane complex, *c*-$C_3H_6 \cdot HCl$ are also given. Comparison shows that from ethene · HCl to MeCP · HCl, the complexation energy of the π complex increases by 2–3 kJ mol^{-1}. In contrast, the complexation energies for **II** and **III** are significantly smaller than for the cyclopropane complex. Evidently, in MeCP the basicity of the π-bond is higher than in ethene, while that of the cyclopropyl ring is lower than in cyclopropane.

The HCl bond lengths R(HCl) in the complexes are calculated to be 1.3016 Å (**I**), 1.2929 Å (**II**) and 1.2915 Å (**III**). In the π complex **I**, R(HCl) is longer by 4.5×10^{-3} Å than in

Table 1 BLYP/6-311++G(d,p) complexation energies, in kJ mol^{-1}, for the complexes of methylenecyclopropane, ethene and cyclopropane with HCl

	ΔE	E_{BSSE}	ΔE_{corr}
MeCP · HCl **I**	−13.38	2.29	−11.09
MeCP · HCl **II**	−7.06	2.05	−5.01
MeCP · HCl **III**	−4.85	1.91	−2.94
MeCP · $(HCl)_2$ **IVa**	−22.63	4.45	−18.18
MeCP · $(HCl)_2$ **IVb**	−18.13	4.30	−13.83
MeCP · $(HCl)_2$ **IVc**	−15.63	4.37	−11.26
MeCP · $(HCl)_2$ **IVd**	−9.36	4.06	−5.30
MeCP · $(HCl)_2$ **IVe**	−7.70	3.83	−3.87
MeCP · $(HCl)_2$ **Va**	−24.92	4.62	−20.30
MeCP · $(HCl)_2$ **Vb**	−16.21	4.27	−11.94
MeCP · $(HCl)_2$ **Vc**	−12.97	4.13	−8.84
$C_2H_4 \cdot HCl$	−10.51	1.52	−8.99
c-$C_3H_6 \cdot HCl$	−9.07	2.07	−7.00
HCl · HCl	−6.59	1.28	−5.31

$C_2H_4 \cdot HCl$, while in **II** and **III** R(HCl) is shorter than in *c*-$C_3H_6 \cdot HCl$, by 1.7×10^{-3} and 3.6×10^{-3} Å, respectively. As the increase in H–Cl bond length upon complexation is proportional to the Van der Waals bond strength, these observations are in line with calculated energies.

The relative populations of complexes **II** and **III** in an equilibrium environment can be estimated from the *ab initio* results if one assumes that the corrections transforming energies into Gibbs energies are similar for the three complexes. The energies in Table 1 then predict that at 100 K, a characteristic temperature in our experiments, the equilibrium populations of **II** and **III** are less than 0.05% that of **I**. Even if we allow for solvent effects, these low fractions suggest that it is unlikely that **II** and **III** can be detected in cryosolutions. It will be discussed below that this is confirmed by our experiments.

It is of interest to compare the structural parameters of complex **I** with those obtained from the Buckingham–Fowler model or the FT-microwave data.[11] The equilibrium geometry of the complex was defined in that study using three quantities: the first is the van der Waals distance R(Y···Cl), where the dummy atom Y is situated at the midpoint of the C=C bond; the other two parameters are ϕ and γ, where ϕ is the angle between the line H···Y and the C=C bond and $(180 - \gamma)$ measures the deviation from linearity of the Y···H–Cl moiety. The values for these quantities have been collected in Table 2. It can be seen that the DFT values compare favorably with the previously reported data. The calculations also support the suggestion[11] of a secondary interaction between the chlorine atom and the hydrogen atoms that are bonded to the carbon atoms 2 and 3 on the same side of the ring as the HCl molecule.

The vibrational frequencies and IR intensities calculated for the 1 : 1 complexes and for the constituent molecules are collected in Table 3. Also given are the complexation shifts $\Delta\nu = \nu_{complex} - \nu_{monomer}$. These data will be used below to identify the experimentally observed complex species.

Table 2 Internal coordinates describing the relative orientation of MeCP and HCl in isomer I

	DFT	B-F[a]	MW[b]
ϕ/degrees	95.6	94	
$180 - \gamma$/degrees	170.8	173	
R(Y···C)/Å	3.608		3.570(2)

[a] Buckingham–Fowler model.[22] [b] Microwave results.[11]

Because of the very weak interaction between the monomers, the vibrations of the complexes can be classified as modes localized in the monomers and as intermolecular modes. The former can unambiguously be correlated with those of the isolated monomers. Therefore, we will describe them using the assignments of the corresponding monomer modes.

Experience with other complexes[24,25] teaches that complexation shifts calculated for isolated complexes are slightly larger than those observed in cryosolutions but that for the larger shifts the predicted sign generally is correct. Therefore, *ab initio* complexation shifts can be used to distinguish between several complexes if the shifts predicted for the different complexes (i) are sufficiently large and (ii) occur in opposite directions. Inspection of Table 3 shows that under these conditions the ν_3, ν_6, ν_{16} and ν_{21} modes of MeCP could lead to the identification of the observed complexes. It may be noted here that, although the C=C bond length is calculated to slightly decrease in complex **III**, its stretching frequency, ν_3, occurs somewhat red shifted. This must be due to differences in the coupling with other modes in the complex and in the monomer.

Table 3 B3LYP/6-311++G(d,p) vibrational frequencies, in cm^{-1}, IR intensities, in km mol^{-1}, and complexation shifts, in cm^{-1}, for MeCP and MeCP · HCl

		MeCP			MeCP · HCl (**I**)				MeCP · HCl (**II**)				MeCP · HCl (**III**)			
Mode	Description	Sym.	ν	Int.	Sym.	ν	Int.	$\Delta\nu$	Sym.	ν	Int.	$\Delta\nu$	Sym.	ν	Int.	$\Delta\nu$
ν_1	=CH_2 stretch	A_1	3119.6	12.7	A′	3117.6	7.1	−2.0	A_1	3122.8	11.0	3.2	A′	3123.6	8.6	4.0
ν_2	*c*-CH_2 stretch	A_1	3100.6	13.7	A′	3103.0	6.6	2.4	A_1	3096.3	10.3	−4.3	A′	3101.8	11.9	1.2
ν_3	C=C stretch	A_1	1827.4	10.1	A′	1811.9	19.9	−15.5	A_1	1831.6	9.8	4.2	A′	1823.5	7.8	−3.9
ν_4	CH_2 scissors	A_1	1482.0	0.1	A′	1481.3	0.1	−0.7	A_1	1480.5	0.1	−1.5	A′	1485.3	0.8	3.3
ν_5	CH_2 scissors	A_1	1442.2	0.9	A′	1442.0	2.2	−0.2	A_1	1442.1	2.0	−0.1	A′	1446.4	2.0	4.2
ν_6	C–C stretch	A_1	1060.0	3.7	A′	1060.4	3.1	0.4	A_1	1056.7	20.5	−3.3	A′	1058.1	4.7	−1.9
ν_7	*c*-CH_2 wag	A_1	1029.3	4.4	A′	1035.4	5.9	6.1	A_1	1038.8	0.8	9.5	A′	1029.3	10.7	0.0
ν_8	C–C stretch	A_1	737.5	6.3	A′	736.2	5.6	−1.3	A_1	731.4	12.1	−6.1	A′	734.4	5.0	−3.1
ν_9	*c*-CH_2 stretch	A_2	3170.9	0.0	A″	3175.5	0.1	4.6	A_2	3170.4	0.0	−0.5	A″	3168.6	0.5	−2.3
ν_{10}	*c*-CH_2 twist	A_2	1162.3	0.0	A″	1165.5	0.0	3.2	A_2	1167.0	0.0	4.7	A″	1169.0	0.0	6.7
ν_{11}	CH_2 twist	A_2	955.2	0.0	A″	959.9	0.0	4.7	A_2	965.2	0.0	10.0	A″	959.9	0.1	4.7
ν_{12}	CH_2 rock	A_2	616.3	0.0	A″	635.0	0.3	18.7	A_2	625.1	0.0	8.8	A″	617.5	0.0	1.2
ν_{13}	*c*-CH_2 stretch	B_1	3183.6	15.5	A′	3187.9	8.4	4.3	B_1	3181.9	7.6	−1.7	A″	3183.7	9.4	0.1
ν_{14}	*c*-CH_2 twist	B_1	1094.0	1.8	A′	1098.5	3.1	4.5	B_1	1104.8	1.4	10.8	A″	1094.6	1.9	0.6
ν_{15}	=CH_2 wag	B_1	920.0	49.4	A′	932.6	74.0	12.6	B_1	927.2	47.8	7.2	A″	930.7	44.2	10.7
ν_{16}	*c*-CH_2 rock	B_1	754.0	2.6	A′	749.1	3.3	−4.9	B_1	758.6	2.7	4.6	A″	771.2	2.2	17.2
ν_{17}	C=CH_2 wag	B_1	290.8	5.3	A′	302.0	6.6	11.2	B_1	316.0	0.2	25.2	A″	301.9	9.8	11.1
ν_{18}	=CH_2 stretch	B_2	3199.7	11.8	A″	3200.6	6.2	0.9	B_2	3204.6	8.9	4.9	A′	3203.6	8.5	3.9
ν_{19}	*c*-CH_2 stretch	B_2	3099.6	16.2	A″	3102.2	9.0	2.6	B_2	3095.9	8.3	−3.7	A′	3092.5	10.9	−7.1
ν_{20}	*c*-CH_2 scissors	B_2	1446.8	2.8	A″	1445.1	5.0	−1.7	B_2	1447.0	2.1	0.2	A′	1447.7	2.3	0.9
ν_{21}	=CH_2 rock	B_2	1138.0	7.1	A″	1142.5	7.1	4.5	B_2	1135.0	7.1	−3.0	A′	1135.8	12.0	−2.2
ν_{22}	*c*-CH_2 wag	B_2	1068.8	1.9	A″	1074.0	1.5	5.2	B_2	1067.1	1.1	−1.7	A′	1079.4	5.0	10.6
ν_{23}	C–C stretch	B_2	898.6	15.9	A″	900.0	14.0	1.4	B_2	901.2	14.7	2.6	A′	891.7	27.1	−6.9
ν_{24}	C=CH_2 rock	B_2	356.5	0.4	A″	354.3	0.2	−2.2	B_2	369.0	0.0	12.5	A′	364.2	0.5	7.7
ν_{HCl}[a]					A′	2730.2	630.3	−205.6	A_1	2856.9	341.8	−78.9	A′	2878.4	207.6	−57.4
ν_{vdW}					A′	385.3	13.8		B_2	260.1	22.4		A′	233.8	23.2	
ν_{vdW}					A″	379.3	20.7		B_1	250.0	31.9		A″	136.5	22.1	
ν_{vdW}					A′	101.9	4.2		A_1	68.1	1.5		A′	65.5	1.2	
ν_{vdW}					A″	44.3	0.2		B_2	52.1	1.1		A′	49.0	0.4	
ν_{vdW}					A′	37.1	0.8		B_1	35.0	1.1		A″	26.4	0.1	

[a] The HCl stretching frequency and IR intensity for monomer HCl are 2935.8 cm^{-1} and 31.7 km mol^{-1}, respectively.

For the 1 : 2 complexes, two different types have been considered, one in which both HCl molecules are bonded to MeCP and the other in which the second HCl is bonded to the first. The calculations converged into five different isomers of the former, and three of the latter type. Their structures are shown in Fig. 2, their energies have been collected in Table 1.

The complexation energies of the complexes of the first type, isomers **IVa**–**IVe**, are significantly smaller than the sum of the values of the corresponding 1 : 1 complexes. This shows that an anti-cooperative effect is active that weakens the van der Waals bonds in these 1 : 2 complexes. As a consequence, in these complexes the van der Waals bonds are systematically longer than in the corresponding 1 : 1 complexes, while the H–Cl bonds are shorter.

The complexation energies for the second type, isomers **Va**–**Vc**, are larger than the sum of the complexation energies of the corresponding 1 : 1 complexes and of $(HCl)_2$. Therefore, in this type of complex a cooperative effect is active, that strengthens the van der Waals bonds. The cooperative effect also shows in the lengths of the H–Cl and of the van der Waals bonds, the former being larger in the 1 : 2 complexes, the latter smaller than the corresponding bonds in the 1 : 1 complexes.

The energies in Table 1 indicate that isomer **Va** is the global minimum for the 1 : 2 complexes, followed by isomer **IVa**, whose energy is 2.1 kJ mol^{-1} above that of **Va**. The energies of the other isomers are at least 6 kJ mol^{-1} higher than that of **Va**. Making the same assumption as above, and taking into account the appropriate statistical weights, these data predict that the relative populations for isomers **Va** and **IVa** are 96.7% and 3.2%, respectively, and that the sum of the relative populations of the other isomers is below 0.1%.

In Table S2 and Table S3 of the supplementary material† the calculated vibrational frequencies, IR intensities and complexation shifts obtained for the 1 : 2 complexes have been collected. In view of the further discussion it is useful to remark that for isomer **Va**, the HCl stretching frequencies are predicted at 2624.9 and 2818.1 cm^{-1}, with intensities 944.0 and 291.3 km mol^{-1}, respectively, while for complex **IVa** the HCl stretching frequencies are predicted at 2758.6 and 2776.3 cm^{-1} with intensities 1018.1 and 19.3 km mol^{-1}, respectively.

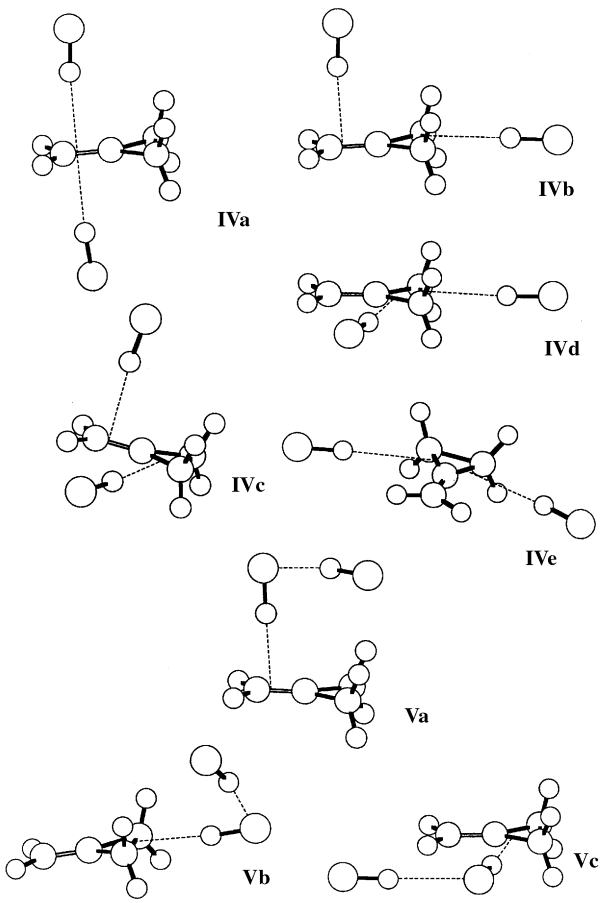

Fig. 2 B3LYP/6-311++G(d,p) equilibrium geometries for the different 1 : 2 complexes formed between MeCP and HCl.

B. Vibrational spectra

The vibrational spectra of HCl and MeCP in liquefied inert gases have been described elsewhere.[26,27] These MeCP monomer assignments are based on those reported for the vapor phase[28–31] and on the calculated frequencies, which are summarized in Table 3.

Compared with the spectra of the monomers, in the spectra of MeCP–HCl mixtures in LAr a significant number of new bands are observed. Their presence signals the formation of weakly bound complexes between MeCP and HCl. The observed frequencies, their assignments and the complexation shifts are summarized in Tables 4 and 5.

In Fig. 3A, the HCl stretching region of spectra recorded at different temperatures from a solution in LAr that contains mole fractions of approximately 2.0×10^{-4} of HCl and 0.2×10^{-4} of MeCP are compared with those of solutions containing only MeCP or HCl. For the mixed solutions, apart from the monomer bands and the bands at 2828 and 2797 cm^{-1}, which are due to $(HCl)_2$ and $(HCl)_3$,[26] respectively, an intense band is observed near 2710 cm^{-1}. This band is assigned to a 1 : 1 complex MeCP · HCl. At lower temperatures other complex bands become more clearly visible, at 2631, 2745 and 2762 cm^{-1}. We assign these bands to 1 : 2 complexes MeCP · $(HCl)_2$. The proposed stoichiometries are confirmed by concentration-dependent studies, to be described in a later paragraph.

As only the 2710 cm^{-1} band can be assigned to a 1 : 1 complex, it must be concluded that only a single 1 : 1 complex

Table 4 Observed vibrational frequencies, in cm^{-1}, and complexation shifts, in cm^{-1}, for MeCP · HCl in LAr at 100 K. [Abbreviations: vs very strong; s strong; m medium; w weak, vw very weak]

	MeCP		MeCP · HCl	
Mode	frequency	Int.	frequency	shift
ν_1	3006.0	5	3002.0	−4.0
ν_3	1739.6	s	1736.5	−3.1
ν_4	1435.9	w	1435.8	−0.1
ν_5	1408.4	m	1409.8	1.4
ν_6	1032.6	s	1034.0	1.4
ν_7	1001.9	s	1005.9	4.0
ν_8	724.5	s	723.9	−0.6
ν_{13}	3067.5	s	3070.2	2.7
ν_{14}	1071.4	m	1075.0	3.6
ν_{15}	888.0	vs	899.6	11.6
ν_{16}	748.5	m	745.3	−3.2
ν_{17}	283.8	s	291.9	8.1
ν_{18}	3083.5	s	3081.1	−2.4
ν_{19}	2995.1	s	2996.9	1.8
ν_{20}	1411.6	m	1411.9	0.3
ν_{21}	1123.1	s	1126.3	3.2
ν_{22}	1045.0	m	1048.6	3.6
ν_{23}	894.2	s	891.1	−3.1
$\nu_4 + \nu_{21}$	2546.2	vw	2549.0	2.8
$2\nu_{21}$	2242.5	w	2248.9	6.4
$\nu_{21} + \nu_{22}$	2166.5	vw	2173.3	6.8
$\nu_7 + \nu_{21}$	2124.2	vw	2131.7	7.5
$2\nu_{22}$	2084.6	w	2092.0	7.4
$\nu_6 + \nu_{22}$	2074.0	w	2079.0	5.0
$\nu_7 + \nu_{22}$	2039.6	w	2047.0	7.4
$2\nu_7$	1975.7	vw	1983.1	7.4
$2\nu_{15}$	1777.5	s	1791.5	14.0
$\nu_8 + \nu_{22}$	1764.9	w	1768.1	3.2

Table 5 Observed vibrational frequencies, in cm^{-1}, and complexation shifts, in cm^{-1}, for the complexes between MeCP and HCl in Lar at 100 K

	Monomer	MeCP · HCl(**I**)		MeCP · $(HCl)_2$ (**IVa**)		MeCP · $(HCl)_2$ (**Va**)			
	ν	ν	$\Delta\nu$	ν	$\Delta\nu$	ν	$\Delta\nu$	ν	$\Delta\nu$
ν_{HCl}	2870.0	2710.5	−159.5	2745.1	−124.9	2630.8	−239.2	2762.0	−108.0
ν_{DCl}	2081.0	1967.6	−113.4	1983.0	−98.0	1916.2	−164.8	1990.9	−90.1
ν_3^{MeCP}	1739.6	1736.5	−3.1			1734.9	−4.7		
ν_{15}^{MeCP}	888.0	899.6	11.6	907.4	19.4	901.8	13.8		

is formed in our studies. It will be shown below that this is confirmed for the complex bands due to modes localised in the MeCP moiety. The complexation shift of the 2710 cm^{-1} band is −159.5 cm^{-1}, which is much more than predicted for isomers **II** and **III**, but is less than −205.6 cm^{-1} predicted for isomer **I**. The experience with HCl complexes is that the shift observed in cryosolution is always less than predicted for the isolated complex.[6,24] Therefore, we identify the species that causes the 2710 cm^{-1} band as isomer **I**.

The absence in our spectra of bands due to isomers **II** and **III** of the 1 : 1 complex makes it unlikely that 1 : 2 complexes derived from **II** or **III** are present in measurable quantities. Thus, the only likely candidates are isomers **IVa** and **Va**. Of all the 1 : 2 isomers investigated, only **Va** gives rise to an HCl stretching frequency lower than that of the 1 : 1 complexes. This makes the assignment of the 2631 cm^{-1} band in Fig. 3 to isomer **Va** obvious. This isomer must give rise to a second HCl stretching, which is predicted, with intensity equal to 32% of the low frequency mode, on the high frequency side of ν_{HCl} in isomer **I**. We prefer to assign the 2762 cm^{-1} band to this mode because both in frequency and intensity it is closer to the predicted values. The remaining 1 : 2 band, at 2745 cm^{-1}, is attributed to isomer **IVa**, because this is the other isomer which is likely to occur and because this assignment leads to the best agreement of the observations with the frequencies and intensities calculated for the various 1 : 2 complexes. For instance, the intensity of the second ν_{HCl} in **IVa** is predicted to be less than 2% of that assigned at 2745 cm^{-1}, which, taking into account the weakness of the latter, explains why no band attributable to the second mode has been detected in our spectra.

The complexation behavior of MeCP with DCl was also studied. Monomer MeCP and DCl spectra are compared, in the ν_{DCl} region, with those of a mixed solution in Fig. 3B. Bands assignable to complexes between DCl and MeCP are observed at 1990.9, 1983.0, 1967.6 and 1916.2 cm^{-1}, with intensity pattern similar to that observed for the HCl stretches. Therefore, the assignment of the more intense 1967.6 cm^{-1} band to isomer **I** of the 1 : 1 complexes, the 1990.9 and 1916.2 cm^{-1} bands to the 1 : 2 complex **Va** and the very weak 1983 cm^{-1} band to the 1 : 2 complex **IVa** is straightforward.

It is well known that DCl stretching bands in general are narrower than corresponding HCl bands. This is also true for the MeCP complexes, as can be seen by comparing Fig. 3A and 3B. For instance, the full width at half height (FWHH) of the 1 : 1 band equals 22.1 cm^{-1} in MeCP · HCl and 13.2 cm^{-1} in MeCP · DCl.

Complex bands observed for vibrations of the MeCP moiety are illustrated in Fig. 4–6, where spectra recorded at different temperatures from a solution in LAr containing mole fractions of approximately 1.5×10^{-4} of HCl and 0.5×10^{-4} of MeCP are compared with that of solution of MeCP. The region of the c-CH_2 rocking mode ν_{16} is given in Fig. 4A.

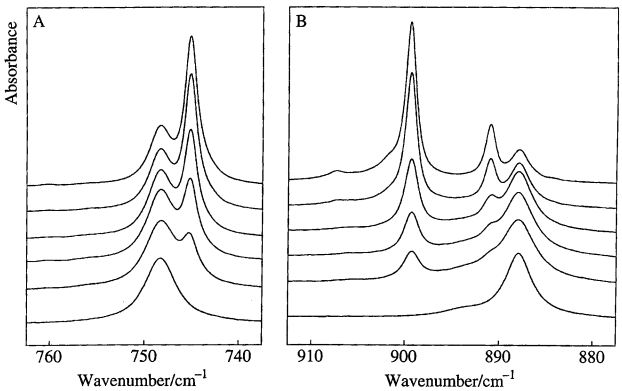

Fig. 4 The ν_{16} region of a solution in LAr containing both MeCP and HCl. From top to bottom, the temperature increases from 98 to 128 K. The lowest trace shows the spectrum of a solution containing only MeCP.

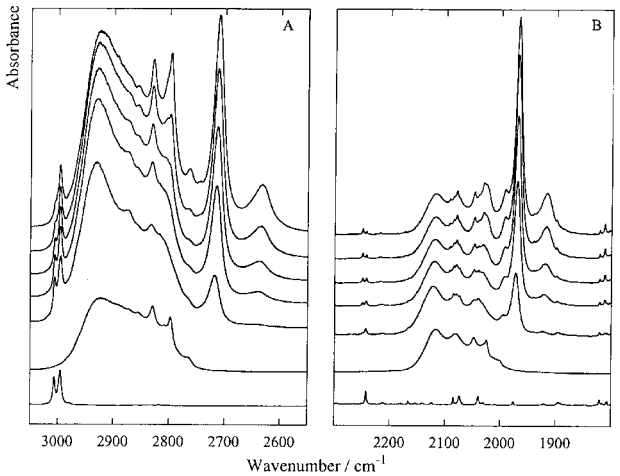

Fig. 3 The HCl (A) and DCl (B) stretching regions for a solution in LAr containing MeCP, HCl and DCl. From top to bottom, the temperature of the solution increases from 98 to 128 K. The lowest two traces show spectra of solutions containing only HCl(DCl) or MeCP.

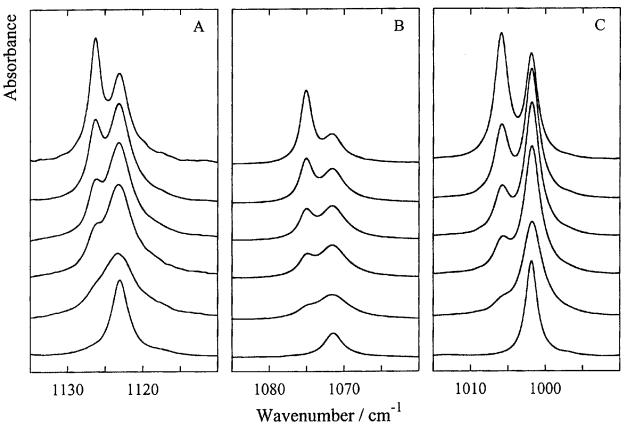

Fig. 5 The ν_{21}(A), ν_{14}(B) and ν_7(C) spectral regions of a solution in LAr containing both MeCP and HCl. From top to bottom, the temperature increases from 98 to 128 K. The lowest trace shows the spectra of a solution containing only MeCP.

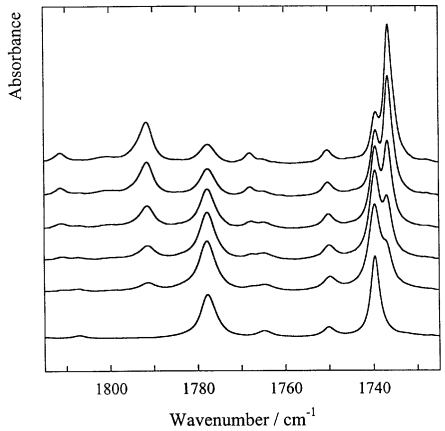

Fig. 6 The C=C stretching region of a solution in LAr containing both MeCP and HCl. From top to bottom, the temperature increases from 98 to 128 K. The lowest trace shows a spectrum of a solution containing only MeCP.

Table 3 shows that in isomers **II** and **III** of the 1 : 1 complex ν_{16} should shift to higher frequencies, by 4.6 and 17.2 cm^{-1}, respectively, but that isomer **I** should shift in opposite direction, by -4.9 cm^{-1}. Fig. 4 clearly illustrates that for the mixed solutions the only complex band occurs on the low frequency side of the monomer band, shifted by -3.2 cm^{-1}. This supports the above conclusion that in our solutions only isomer **I** was present in detectable concentrations.

Around 900 cm^{-1} ν_{15} and ν_{23} must be assigned. As is clear from Fig. 4, two monomer bands are observed in LAr, at 888 and 894 cm^{-1}. Their assignment to ν_{15} and ν_{23}, however, is problematic,[27] because the relative intensities in the doublet observed in LAr are opposite to those in the vapour phase[28] and are also opposite to the calculated ones in Table 3. For the present study we adopt the vapour phase order of assignment, *i.e.* monomer ν_{15} is assigned to the 888 cm^{-1} band, and ν_{23} to the 894 cm^{-1} band. The 1 : 1 complex bands at 899.6 and 891.1 cm^{-1} that are seen in Fig. 4B can then be assigned, consistent with the predictions in Table 3, as ν_{15} and ν_{23}, respectively, of isomer **I**. On the high frequency side of the 899.6 cm^{-1} band two much weaker bands become visible at lower temperatures, at 907.4 and 901.8 cm^{-1}. We assign these bands to 1 : 2 species. The ν_{23} mode in the 1 : 2 complexes is predicted to fall not more than 5 cm^{-1} above the same mode in the 1 : 1 complex, as is clear from Tables S2 and S3 of the supplementary information. Keeping in mind that the predicted complexation shifts tend to be somewhat higher than those observed in cryosolution, neither of the 1 : 2 bands can be assigned to ν_{23}. Therefore, they must both be assigned as ν_{15}, which implies that two different isomers were present in the solution investigated. This is in agreement with the conclusions from the HCl stretching region. Limiting ourselves to the more likely isomers **IVa** and **Va**, Tables S2 and S3† show that in the former ν_{15} should occur some 7 cm^{-1} above ν_{15} in the 1 : 1 complex, while for isomer **Va** it should be quasi-degenerate with the 1 : 1 band. Therefore, we assign the 907.4 cm^{-1} band to ν_{15} in complex **IVa**, and the 901.8 cm^{-1} band to the same mode in isomer **Va**. It must be stressed that in view of the uncertainties in the assignments of monomers ν_{15} and ν_{23}, the assignments of the complex bands must be regarded as tentative.

In Fig. 5 the regions of ν_{21}, ν_{14} and ν_7 are given. Each of these modes appears well separated from other bands in the monomer spectra, and for each a single complex band is present in the spectra of the mixed solutions, illustrating that a single 1 : 1 complex was formed. Comparison with the *ab initio* frequencies in Table 3 shows that the upward shift of the ν_{21} complex band again supports the identification of the complex as isomer **I**. Using ν_{14} or ν_7 the identification can not be made unambiguously, but in both cases the observations agree better with the predictions for isomer **I** than with those for the other.

The region of the C=C stretch, ν_3, is shown in Fig. 6. It was described before that the $v = 1$ level of ν_3 is in Fermi resonance with the $v = 2$ level of ν_{15}.[28–31] In agreement with this, a Fermi doublet is observed, with ν_3 assigned at 1739.6 cm^{-1}, and $2\nu_{15}$ at 1777.5 cm^{-1}. The bands at 1736.4 and 1791.5 cm^{-1} in the spectra of the mixed solution are the corresponding 1 : 1 complex bands. The complexation shift observed for ν_3, -3.1 cm^{-1}, is much smaller than predicted for isomer **I**, -15.5 cm^{-1}, and agrees rather well with that for isomer **III**, -3.9 cm^{-1}. However, this should not be taken as evidence that isomer **III** is formed, as it is clear from Fig. 6 that the complexation shift for $2\nu_{15}$ is much larger, signalling that the Fermi resonance is not the same in monomer and complex. Some insight into this was gained from an analysis of the intensities of ν_3 and $2\nu_{15}$. These were determined by least-squares band fitting of the experimental spectra, using Gauss–Lorentz sum functions. For the monomer, the intensity ratio $I_{\nu_3}/I_{2\nu 15}$ increases, by some 5%, from 1.03 at 96 K, to 1.09 at 118 K, while for the complex it increases, by 34%, from 1.92 to 2.57 over the same temperature range. The temperature dependence of the ratio reflects the change in the solvent influence on the vibrational levels involved. More importantly, the larger intensity ratio for the complex shows that the Fermi resonance is weaker in the complex than in the monomer. In the harmonic approximation the complexation shift of $2\nu_{15}$ is twice that of ν_{15}, the latter predicted at 12.6 cm^{-1}. Combined with the *ab initio* shift for ν_3, the harmonic frequency difference between ν_3 and $2\nu_{15}$ in the complex is predicted to be increased by 40.7 cm^{-1} over that in the monomer. Assuming that the value of the cubic force constant, in terms of the normal coordinates, $F_{3,15,15}$ is not greatly affected by the complexation, this increase must lead to a reduced Fermi resonance in the complex, as is observed. Thus, the $v = 1$ level of ν_3 in the complex is shifted less by the resonance than in the monomer. This, in agreement with observation, causes the complexation shift of the observed ν_3 fundamental to be significantly smaller than the harmonic *ab initio* shift.

At the lowest temperatures studied a feature becomes visible at 1734.9 cm^{-1}. Its intensity follows the pattern observed for the 1 : 2 complex bands in the ν_{HCl} and the ν_{15} regions, and consequently, must also be assigned to the 1 : 2 complexes. The proposed assignment of this band is given in Table 5.

The spectra in Fig. 6 further illustrate that complex bands are observed also for combination bands and overtones. The frequencies of these bands, and their assignment, are given in Table 4, but will not be discussed in detail.

The complex bands observed in the low frequency region are illustrated in Fig. 7. The monomer band at 283.8 cm^{-1} is assigned as ν_{17},[28–31] the corresponding complex band grows in at 291.9 cm^{-1}. The weaker and broader complex band at 310 cm^{-1} is assigned as the high frequency component of the intermolecular modes predicted at 385.3 and 379.3 cm^{-1} for the π complex. The considerable overestimation of the frequency of this mode by the B3LYP calculations is consistent with the behaviour of the similar mode in the HCl complexes of ethene[6] and cyclopropane.[9] In the latter two, the intermolecular doublet was predicted with a frequency difference very close to that of the MeCP complex, while the experimental separation is 45–50 cm^{-1}; it cannot be excluded that for MeCP·HCl the low frequency component is hidden in the low frequency shoulder of the 283.8 cm^{-1} MeCP monomer band.

The B3LYP frequencies in Table 3 for the above intermolecular modes are approximately 85–90 cm^{-1} higher than those predicted for the ethene and cyclopropane complexes.[6] In agreement with this, the 310 cm^{-1} of MeCP·HCl falls

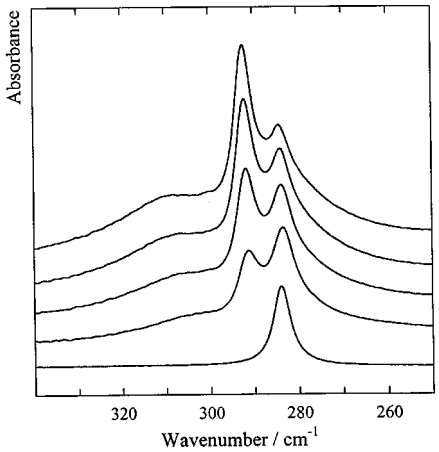

Fig. 7 The 340–250 cm^{-1} region of a solution in LAr containing both MeCP and HCl. From top to bottom, the temperature increases from 98 to 128 K. The lowest trace shows a spectrum of a solution containing only MeCP.

60–70 cm^{-1} higher than the high frequency component of the other two complexes. As these modes involve motions of the monomers with respect to each other, this suggests that MeCP · HCl is the stronger complex. This will be confirmed below by the measured complexation enthalpy.

To complete the analysis, spectra of mixtures dissolved in liquefied nitrogen were also investigated. Again, the formation of 1 : 1 and 1 : 2 complexes was concluded from the appearance of new bands close to the HCl or MeCP monomer bands. Because of the similarity with the argon solutions, no detailed description of these bands will be given. It suffices to note that in liquid nitrogen an intense band due to the HCl stretching fundamental in MeCP · HCl and a much weaker feature due to one of the HCl stretching fundamentals in isomer **Va** can be observed, near 2714 and 2643 cm^{-1}, respectively.

C. Stoichiometry of the observed species

Using the Lambert–Beer law combined with the equilibrium constant for the formation of a complex $(MeCP)_m \cdot (HCl)_n$ from its monomers, and neglecting the frequency dependence of surface and cuvette effects, it is easily shown that the band area of a complex band is linearly related to the product of the mth power of the band area of a band of monomer MeCP and the nth power of the band area of the HCl band. This property was used to establish the stoichiometry of the present complexes. Band areas were determined for spectra, recorded at 110 K, of a series of solutions in which the mole fraction of MeCP varied between 0.2×10^{-4} and 4.0×10^{-4}, and the mole fraction of HCl between 0.6×10^{-4} and 8.0×10^{-4}. For monomer MeCP, the band area of the 1001.9 cm^{-1} band was obtained from least-squares band fitting, using Gauss–Lorentz sum functions. Band areas for the complexes, and for HCl, were determined as follows. A spectrum of HCl in LAr, recorded at the same temperature as the mixtures, was rescaled and subtracted from the spectra of the mixtures. For each solution, the rescaling factor was adjusted to reduce to zero the contribution of monomer HCl in the difference spectrum. The optimized difference spectra were then subjected to least squares band fitting, again using Gauss–Lorentz sum functions. Due to the pronounced asymmetry of the complex bands, an optimal fit required a sum of three functions for the 2710.5 cm^{-1} band, and a sum of two functions for the 2630.8 cm^{-1} band. The sum of the areas of the functions used to simulate each of these multiplets was then used as band area for the corresponding complex. Finally, for each solution the HCl monomer band area was determined by numerical integration of the HCl absorption in the rescaled spectrum used in the subtraction.

Linear regressions were performed between the set of band areas of each complex band, and different products of monomer intensities. The χ^2 values of these regressions are given in Table 6. It can be seen that for the 2710.5 cm^{-1} band the highest degree of linearity is obtained for the product $I_{MeCP} \times I_{HCl}$, from which follows that this band is due to the 1 : 1 complex MeCP · HCl. For the band at 2630.8 cm^{-1} the smallest χ^2 value is found for the product $I_{MeCP} \times (I_{HCl})^2$, so that this band must be due to a complex with 1 : 2 stoichiometry.

The bands at 2745 and 2762 cm^{-1} are relatively weak, and severely overlap with other bands. As a consequence their band areas could not be reliably obtained. Hence, for these bands the proposed stoichiometry is only justified by their qualitative intensity behavior in the concentration series, which is similar to that of the 2630.8 cm^{-1} band.

Table 6 χ^2 values from the stoichiometry analysis of the complexes formed between MeCP and HCl

Proposed stoichiometry	2710.5 cm^{-1}	2630.8 cm^{-1}
MeCP · HCl	0.006	0.049
MeCP · $(HCl)_2$	0.691	0.005
$(MeCP)_2$ · $(HCl)_2$	0.155	0.027
$(MeCP)_2$ · HCl	0.694	0.279

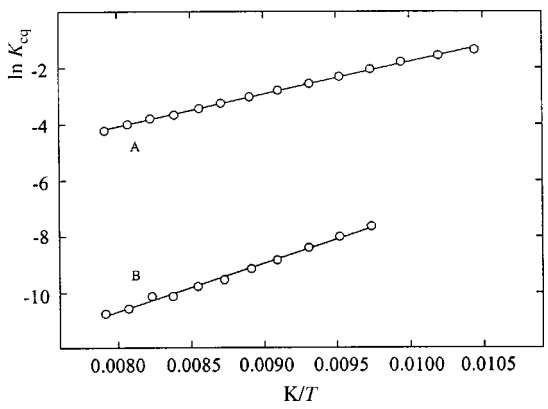

Fig. 8 Van't Hoff plots for the MeCP · HCl complex (A) and the MeCP · $(HCl)_2$ complex (B) observed in LAr.

D. Complexation enthalpies of the observed species

The relative stability of the 1 : 1 and 1 : 2 complexes in LAr was established from a temperature study, in which IR spectra of solutions containing MeCP and HCl, with mole fractions of 0.4×10^{-4} and 2.7×10^{-4}, respectively, were recorded. From these, the complexation enthalpy ΔH° was determined using the Van't Hoff isochore. In this method, ΔH° is obtained as the slope of the plot obtained by plotting, the logarithm of the equilibrium constant, expressed in terms of band areas of IR bands of the species involved, against the inverse temperature.[32] Band areas for monomer and complex bands were derived for the same bands, using the same procedures, as in the concentration study discussed above. The Van't Hoff plots derived from these are shown in Fig. 8. From the slope of the linear regressions through the experimental points, corrected for the density variations of the solution,[32,33] the complexation enthalpies for the 1 : 1 complex and the most stable 1 : 2 complex (**Va**) were calculated to be −9.9(3) and −14.6(4) kJ mol^{-1}, respectively. For the same reasons as above, ΔH° for the other 1 : 2 complex, **IVa**, could not be established.

Discussion

The observed 1 : 1 complex bands have frequencies compatible with the *ab initio* predictions for the π complex **I**, from

which we conclude that in the cryosolutions the π complex is formed. Careful inspection of the regions in which diagnostic bands due to complex **II** or **III** were predicted gave no evidence for the presence of even the weakest transition. Thus, in agreement with the *ab initio* predictions, the complexation energies of the secondary complexes **II** and **III** must be significantly smaller than that of isomer **I**.

As was mentioned in the Introduction, the MeCP/HCl complex has also been detected in a matrix isolation IR study. Based on general characteristics of the spectra, the authors proposed that the π complex was present in the matrix. Apart from bands in the HCl stretching region, in the matrix study complex bands associated with the MeCP fundamentals at 286 (ν_{17}), 748 (ν_{16}), 886 (ν_{15}) and 1120 cm^{-1} (ν_{21}) were reported.[10] Comparison of these argon matrix monomer frequencies with the solution values in Table 4 shows that, in agreement with expectation, the transition from liquid to solid argon shifts the vibrational frequencies by not more than a few wavenumbers. A similar trend should be observed for the MeCP modes of the 1 : 1 complex: for ν_{15} and ν_{21} this is the case, with the complex bands detected in the matrix at 900 and 1125 cm^{-1} and those in LAr at 899.6 and 1126.3 cm^{-1}. For ν_{16} and ν_{17}, however, the LAr data disagree with the matrix data. Fig. 4 clearly illustrates the red shift of ν_{16} by 3.2 cm^{-1}, while for the matrix a band blue shifted by 10 cm^{-1} is reported. Similarly, Fig. 7 shows that in LAr the complex band is blue shifted, by 8.1 cm^{-1}, while in the matrix a band red shifted by 26 cm^{-1} is assigned to the complex. It is quite unlikely that such discrepancies are caused by the differences in the surroundings of the complex species. A possible explanation would be that in the matrix a different isomer of the complex was detected. Inspection of Table 3 shows that the complex bands observed for ν_{15} and ν_{16} are compatible with this explanation, but that those observed for ν_{17} and ν_{21} are shifted in a direction opposite to that predicted for isomers **II** and **III**, while the matrix complexation shift of ν_{HCl}, −171 cm^{-1}, points to the π complex. Upon annealing of the matrix, a complex band at 889 cm^{-1} appeared, which was found to grew in more rapidly at relatively high HCl concentration than the other complex bands.[10] Although not explicitly interpreted by the authors, such behaviour is suggestive of the fact that the 889 cm^{-1} band belongs to a species with a diffferent stoichiometry. However, in LAr, the band at 891.1 cm^{-1}, which most likely corresponds to the 889 cm^{-1} matrix band, can be clearly identified as due to the 1 : 1 species. The proper interpretation of this and the previous discrepancy probably awaits a re-investigation of the matrix spectra.

The important number of fundamental complex bands observed in this study allows a quantitative appreciation of the use of B3LYP/6-311++G(d,p) predictions for comparison with cryosolution data. To this end, in Fig. 9 the predicted shifts are plotted against the corresponding observed values. It can be seen that, with one exception, a good correlation is found. The exception is ν_3. As discussed above, this is the consequence of the Fermi resonance that disturbs this fundamental.

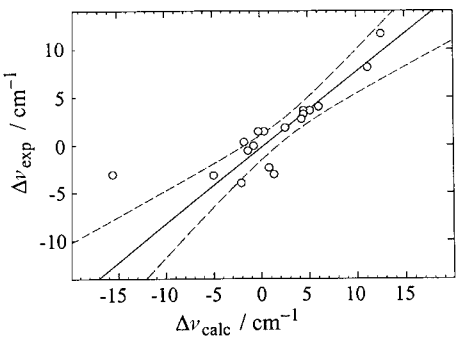

Fig. 9 Comparison of the experimental complexation shifts $\Delta\nu = \nu_{complex} - \nu_{monomer}$ for MeCP · HCl complex with the theoretical values derived from the B3LYP/6-311++G(d,p) calculations. The solid line and the dashed lines refer to the linear regression line and the 99% confidence interval, respectively.

The linear regression line and the 99% confidence interval, obtained by using all data except that for ν_3, are also shown in Fig. 9. The constants of the linear regression $\Delta\nu_{exp} = a\,\Delta\nu_{calc} + b$ are $a = 0.8(2)$ and $b = -0.3(9)$ cm^{-1} while the correlation coefficient equals 0.91. It is interesting to note that the regression line, within the limits of uncertainty, passes through the origin of the plot, which is in agreement with expectations. The value of the direction cosine confirms what was stated earlier, namely that the calculated complexation shifts are somewhat larger than the observed values. This, again, is in good agreement with previous experience.

A quantity of interest in the characterization of a complex is the complexation energy of the isolated species. It can be obtained from the complexation enthalpy in solution by correcting for solvation effects and for thermal and zero-point vibrational contributions. In this study the free enthalpies of solvation $\Delta_{sol}G$ for the monomers and for MeCP · HCl (**I**) and MeCP · $(HCl)_2$ (**Va**) were obtained from free energy perturbation theory[34–36] calculations, using BOSS 4.1.[37] From these, the solvation enthalpy difference, $\Delta_{sol}H$, and solvation entropy difference, $\Delta_{sol}S$, were extracted using a finite difference method similar to that described in ref. 37. For all calculations, the solute–solvent interactions were modeled using the OPLS all-atom potential functions[38] included in BOSS 4.1. The resulting enthalpies and entropies are given in Table 7.

From the data in Table 7 it follows that the complexation enthalpies in LAr are smaller than the vapor phase value, by 3.24(50) kJ mol^{-1} for MeCP · HCl and 7.14(57) kJ mol^{-1} for MeCP · $(HCl)_2$. Correction of the liquid phase ΔH° with these values results in a vapor phase complexation enthalpy ΔH°_{vapor} of −13.1(6) kJ mol^{-1} for MeCP · HCl and −21.7(7) kJ mol^{-1} for MeCP · $(HCl)_2$. In a next step, statistical thermodynamics[39] was applied to transform the vapor phase enthalpies into energies. For all species the zero-point vibrational energies were calculated using the B3LYP/6-311++G(d,p) *ab initio* frequencies. The thermal contributions were calculated at the mid-point of the temperature range in which ΔH° was determined. Translational and rotational thermal contributions were calculated in the classical limit and vibrational thermal contributions were calculated in the harmonic approximation using the same frequencies as for the zero-point corrections. These calculations result in a correction of −3.78 kJ mol^{-1} for the 1 : 1 complex and −6.96 kJ mol^{-1} for the 1 : 2 complex. Applying these to the ΔH°_{vapor} yields an 'experimental' complexation energy ΔE_{exp} of −16.9(12) kJ mol^{-1} for MeCP · HCl and −28.7(14) kJ mol^{-1} for MeCP · $(HCl)_2$, with the uncertainties being, somewhat arbitrarily, chosen to be twice the value for ΔH° to account for the approximations made in transforming ΔH° to ΔE_{exp}.

The B3LYP/6-311++G(d,p) complexation energies for MeCP · HCl and MeCP · $(HCl)_2$ are −13.4 and −24.9 kJ mol^{-1}, respectively. Both are smaller than the corresponding experimental value. Correction for BSSEs results in complexation energies of 11.1 kJ mol^{-1} for MeCP · HCl and −20.3 kJ mol^{-1} for MeCP · $(HCl)_2$, which are even further away from

Table 7 Solvation enthalpies, in kJ mol^{-1} and solvation entropies, in J K^{-1} mol^{-1} calculated using free energy perturbation theory

Species	$\Delta_{sol}H$	$\Delta_{sol}S$
HCl	−9.64(21)	−35.0(18)
MeCP	−24.95(31)	−90.7(26)
$(HCl)_2$	−18.54(18)	−69.2(16)
MeCP · HCl (**I**)	−31.35(33)	−114.5(29)
MeCP · $(HCl)_2$ (**Va**)	−37.09(38)	−133.2(34)

the experimental values. These data confirm earlier observations that at the B3LYP/6-311++G(d,p) level the stability of weakly bound complexes is often seriously underestimated.

More accurate *ab initio* energies were obtained in the following way. For each species, using the DFT geometry, single-point calculations were made at the MP2 = full/aug-cc-PVTZ level. The complexation energies obtained, before and after correction for BSSE, are -27.5 and -19.4 kJ mol^{-1} for the 1 : 1 complex and -47.2 and -32.4 kJ mol^{-1} for the 1 : 2 complex. Clearly, the uncorrected complexation energies seriously overestimate the experimental values, while the corrected values agree rather well.

The difference between the complexation energies for MeCP·HCl and MeCP·(HCl)$_2$ reflects the energetics of binding a HCl molecule to the HCl already present. The energy involved must be compared with the complexation energy for the HCl dimer, in which a similar bond is present. For the latter, the complexation enthalpy ΔH° in liquid argon, corrected for the density variation of the solvent, was found to be $-4.2(3)$ kJ mol^{-1}.[6] Using the same procedures as above, a solvation enthalpy difference of $-0.74(35)$ kJ mol^{-1}, and a dynamic contribution of 2.41 kJ mol^{-1} are calculated. From these, the experimental complexation energy for the HCl dimer is determined to be $-7.3(10)$ kJ mol^{-1}. This value is significantly smaller than the difference of $-11.8(17)$ kJ mol^{-1} between the complexation energies for MeCP·HCl and MeCP·(HCl)$_2$, which shows that in the 1 : 2 complex an important cooperative effect of $11.8(17) - 7.3(10) = 4.5(19)$ kJ mol^{-1} must be active. The BSSE corrected value at the MP2 level for this quantity, 5.7 kJ mol^{-1}, compares favorably with the experimental value.

Finally, it may be noted that the 'experimental' complexation energy for the 1 : 1 complex, $-16.9(12)$ kJ mol^{-1}, is noticeably larger than the values of $-14.0(6)$ and $-14.6(6)$ kJ mol^{-1} obtained for ethene·HCl and cyclopropane·HCl, respectively.[9]

Acknowledgement

W.A.H. thanks the Fund for Scientific Research (FWO-Vlaanderen) for an appointment as Postdoctoral Fellow. The FWO is also thanked for help towards the spectroscopic equipment used in this study. The authors thank the Flemish Community for financial support through the Bilateral Cooperation between Flanders and Poland.

Supplementary material available

Table S1 reports the B3LYP/6-311++G(d,p) equilibrium geometries for the 1 : 1 and 1 : 2 complexes formed between MeCP and HCl. Tables S2 and S3 contain the B3LYP/6-311++G(d,p) vibrational frequencies, infrared intensities and complexation shifts for the 1 : 2 complexes MeCP·(HCl)$_2$ of the type **IV** and **V** respectively. Table S4 gives characteristic vibrational frequencies for MeCP dissolved in LAr, at 100 K, and in the vapor phase.

References

1 A. J. Barnes, *J. Mol. Struct.*, 1983, **100**, 259.
2 A. J. Barnes, H. E. Hallam and G. F. Scrimshaw, *Trans. Faraday Soc.*, 1969, **69**, 3172.
3 P. D. Aldrich, A. C. Legon and W. H. Flygare, *J. Chem. Phys.*, 1981, **75**, 2126.
4 S. G. Kukolich, P. D. Aldrich, W. G. Read and E. J. Campbell, *J. Chem. Phys.*, 1983, **79**, 1105.
5 K. G. Tokhadze and N. A. Tkhorzhevskaya, *J. Mol. Struct.*, 1992, **270**, 351.
6 W. A. Herrebout, G. P. Everaert, B. J. Van der Veken and M. O. Bulanin, *J. Chem. Phys.*, 1997, **107**, 8886.
7 L. W. Buxton, P. D. Aldrich, J. A. Shea, A. C. Legon and W. H. Flygare, *J. Chem. Phys.*, 1981, **75**, 2681.
8 C. E. Truscott and B. S. Ault, *J. Phys. Chem.*, 1984, **88**, 2323.
9 G. P. Everaert, W. A. Herrebout and B. J. Van der Veken, *J. Mol. Struct.*, 2000, in press.
10 C. E. Sass and B. S. Ault, *J. Phys. Chem.*, 1987, **91**, 3207.
11 Z. Kisiel, P. W. Fowler and A. C. Legon, *J. Chem. Phys.*, 1994, **101**, 4635.
12 Z. Kisiel, P. W. Fowler and A. C. Legon, *Chem. Phys. Lett.*, 1995, **232**, 187.
13 A. C. Legon and D. G. Lister, *Phys. Chem. Chem. Phys.*, 1999, **1**, 4175.
14 K. G. Tokhadze, in *Molecular Cryospectroscopy*, ed. R. J. H. Clark and R. E. Hester, Wiley and Sons, Chichester, 1995, ch. 5.
15 B. J. Van der Veken, in *Low Temperature Molecular Spectroscopy*, ed. R. Fausto, Kluwer Academic Publishers, Dordrecht, 1996, p. 371.
16 V. V. Bertsev, in ref. 14, ch. 1.
17 M. J. Frisch, G. W. Trucks, H. B. Schlegel, P. M. W. Gill, B. G. Johnson, M. A. Robb, J. R. Cheeseman, T. Keith, G. A. Petersson, J. A. Montgomery, K. Raghavachari, M. A. Al-Laham, V. G. Zakrzewski, J. V. Ortiz, J. B. Foresman, J. Cioslowski, B. B. Stefanov, A. Nanayakkara, M. Challacombe, C. Y. Peng, P. Y. Ayala, W. Chen, M. W. Wong, J. L. Andres, E. S. Replogle, R. Gomperts, R. L. Martin, D. J. Fox, J. S. Binkley, D. J. Defrees, J. Baker, J. P. Stewart, M. Head-Gordon, C. Gonzalez and J. A. Pople, *GAUSSIAN 94, Revision E4*, Pittsburgh, 1996.
18 A. D. Becke, *J. Chem. Phys.*, 1993, **98**, 5648.
19 C. Lee, W. Yang and R. G. Parr, *Phys. Rev. B*, 1998, **37**, 785.
20 S. F. Boys and F. Bernardi, *Mol. Phys.*, 1970, **19**, 553.
21 S. A. Peebles and R. L. Kuczkowski, *J. Mol. Struct.*, 1998, **447**, 151.
22 A. D. Buckingham and P. W. Fowler, *J. Chem. Phys.*, 1983, **79**, 6426.
23 A. D. Buckingham and P. W. Fowler, *Can. J. Chem.*, 1985, **63**, 2018.
24 W. A. Herrebout and B. J. Van der Veken, *J. Phys. Chem.*, 1996, **100**, 15695.
25 W. A. Herrebout, J. Lundell and B. J. Van der Veken, *J. Phys. Chem. A*, 1998, **102**, 10173.
26 B. J. Van der Veken and F. R. De Munck, *J. Chem. Phys.*, 1992, **97**, 3060.
27 W. A. Herrebout, R. Szostak and B. J. Van der Veken, *J. Phys. Chem.*, 2000, in the press.
28 J. E. Bertie and M. G. Norton, *Can. J. Chem.*, 1970, **48**, 3889.
29 J. E. Bertie and M. G. Norton, *Can. J. Chem.*, 1971, **49**, 2229.
30 R. W. Mitchell and J. A. Merritt, *Spectrochim. Acta, Part A*, 1971, **27**, 1609.
31 C. J. Wurrey and A. B. Nease, in *Vibrational Spectra and Structure*, ed. J. R. Durig, Elsevier, Amsterdam, 1978, vol. 7, ch. 1.
32 B. J. Van der Veken, *J. Phys. Chem.*, 1996, **100**, 17436.
33 V. V. Bertsev, N. S. Golubev and D. N. Shchepkin, *Opt. Spektrosk.*, 1976, **40**, 951.
34 N. A. McDonald, E. M. Duffy and W. L. Jorgensen, *J. Am. Chem. Soc.*, 1998, **120**, 5104.
35 C. Jenson, J. Liu, K. N. Houk and W. L. Jorgensen, *J. Am. Chem. Soc.*, 1997, **119**, 12982.
36 G. A. Kaminski and W. L. Jorgensen, *J. Phys. Chem. B*, 1998, **102**, 1787.
37 W. L. Jorgensen, *BOSS, version 4.1*, Yale University, New Haven, CT, 1999.
38 W. L. Jorgensen, D. S. Maxwell and J. Tirado-Rives, *J. Am. Chem. Soc.*, 1996, **118**, 11225.
39 D. A. McQuarrie, *Statistical Mechanics*, University Science Books, Sausolito, CA, 2000.